

Mechanism-based classification of PAH mixtures to predict carcinogenic potential

The Faculty of Oregon State University has made this article openly available.
Please share how this access benefits you. Your story matters.

Citation	Tilton, S. C., Siddens, L. K., Krueger, S. K., Larkin, A. J., Löhr, C. V., Williams, D. E., ... & Waters, K. M. (2015). Mechanism-based classification of PAH mixtures to predict carcinogenic potential. <i>Toxicological Sciences</i> , 146(1), 135-145. doi:10.1093/toxsci/kfv080
DOI	10.1093/toxsci/kfv080
Publisher	Oxford University Press
Version	Accepted Manuscript
Terms of Use	http://cdss.library.oregonstate.edu/sa-termsfuse

1
2
3 1 Mechanism-based classification of PAH mixtures to predict carcinogenic potential
4
5
6 2

7
8 3 Susan C. Tilton^{*,†,1}, Lisbeth K. Siddens^{*,†}, Sharon K. Krueger^{*,‡}, Andrew J. Larkin^{*,†},
9

10 4 Christiane V. Löhr[§], David E. Williams^{*,†,‡}, William M. Baird^{*,†}, Katrina M. Waters^{*,¶}
11
12
13 5

14
15 6 * Superfund Research Center, [†] Environmental and Molecular Toxicology Department, [‡] Linus
16

17 7 Pauling Institute, [§] College of Veterinary Medicine, Oregon State University, Corvallis, OR,
18

19 8 97331; [¶] Biological Sciences Division, Pacific Northwest National Laboratory, Richland, WA,
20

21 9 99352
22
23
24
25 10

26
27 11 ¹ To whom correspondence should be addressed at Environmental and Molecular Toxicology
28

29 12 Department, Oregon State University, Corvallis, OR 97331. Tel: 541-737-1740. Fax: 541-737-
30

31 13 0497. Email: susan.tilton@oregonstate.edu
32
33
34 14

35
36 15 Author emails:
37

38
39 16 Susan C. Tilton: susan.tilton@oregonstate.edu
40

41 17 Lisbeth K. Siddens: siddensb@onid.oregonstate.edu
42

43 18 Sharon K. Krueger: sharon.krueger@oregonstate.edu
44

45
46 19 Andrew J. Larkin: larkinan@onid.orst.edu
47

48 20 Christiane V. Löhr: christiane.loehr@oregonstate.edu
49

50 21 David E. Williams: david.williams@oregonstate.edu
51

52 22 William M. Baird: william.baird@oregonstate.edu
53

54
55 23 Katrina M. Waters: katrina.waters@pnnl.gov
56
57
58
59
60

1
2
3
4
5
6
7
8
9
10
11
12
13
14
15
16
17
18
19
20
21
22
23
24
25
26
27
28
29
30
31
32
33
34
35
36
37
38
39
40
41
42
43
44
45
46
47
48
49
50
51
52
53
54
55
56
57
58
59
60

24

25 Running Title: Pathway-based prediction of PAH tumors

1
2
3 26 **Abstract**
4
5
6 27
7

8 28 We have previously shown that relative potency factors and DNA adduct measurements are
9
10 29 inadequate for predicting carcinogenicity of certain polycyclic aromatic hydrocarbons (PAHs)
11
12 30 and PAH mixtures, particularly those that function through alternate pathways or exhibit greater
13
14 31 promotional activity compared to benzo[*a*]pyrene (BaP). Therefore, we developed a pathway-
15
16 32 based approach for classification of tumor outcome after dermal exposure to PAH/mixtures.
17
18 33 FVB/N mice were exposed to dibenzo[*def,p*]chrysene (DBC), BaP or environmental PAH
19
20 34 mixtures (Mix 1-3) following a two-stage initiation/promotion skin tumor protocol. Resulting
21
22 35 tumor incidence could be categorized by carcinogenic potency as
23
24 36 DBC>>BaP=Mix2=Mix3>Mix1=Control, based on statistical significance. Gene expression
25
26 37 profiles measured in skin of mice collected 12 h post-initiation were compared to tumor outcome
27
28 38 for identification of short-term bioactivity profiles. A Bayesian integration model was utilized to
29
30 39 identify biological pathways predictive of PAH carcinogenic potential during initiation.
31
32 40 Integration of probability matrices from four enriched pathways ($p<0.05$) for DNA damage,
33
34 41 apoptosis, response to chemical stimulus and interferon gamma signaling resulted in the highest
35
36 42 classification accuracy with leave-one-out cross validation. This pathway-driven approach was
37
38 43 successfully utilized to distinguish early regulatory events during initiation prognostic for tumor
39
40 44 outcome and provides proof-of-concept for using short-term initiation studies to classify
41
42 45 carcinogenic potential of environmental PAH mixtures. These data further provide a ‘source-to-
43
44 46 outcome’ model that could be used to predict PAH interactions during tumorigenesis and provide
45
46 47 an example of how mode-of-action based risk assessment could be employed for environmental
47
48 48 PAH mixtures.
49
50
51
52
53
54
55
56
57
58
59
60

1
2
3 49
4
5
6 50
7
8
9
10
11
12
13
14
15
16
17
18
19
20
21
22
23
24
25
26
27
28
29
30
31
32
33
34
35
36
37
38
39
40
41
42
43
44
45
46
47
48
49
50
51
52
53
54
55
56
57
58
59
60

Key words: polycyclic aromatic hydrocarbons, toxicogenomics, modeling, skin cancer, mixtures

51 Introduction

52 Polycyclic aromatic hydrocarbons (PAHs) are a class of over 1500 chemicals formed as
53 incomplete combustion products and released into the environment from both natural (e.g. forest
54 fires) or anthropogenic (e.g. burning of fossil fuels, tobacco, charbroiled meats) sources. Several
55 PAHs, particularly those with more than four rings such as benzo[a]pyrene (BaP),
56 dibenzo[def,p]chrysene (DBC), have been designated as Class 1 known or Class 2A probable
57 human carcinogens by the International Agency for Research on Cancer (IARC, 2010). While
58 much of the research on PAH carcinogenicity focuses on individual PAHs and BaP, in particular,
59 most human exposures to PAHs result from chemical mixtures through dietary, inhalation or
60 dermal routes of exposure. Primary sources of environmental exposure to these PAHs include
61 wood smoke, creosote and burning of fossil fuels and tobacco (IARC, 2010). Recently, diesel
62 engine exhaust was added to the list of Class 1 known human carcinogens and certain other
63 PAH-containing mixtures, including air pollution, have been designated as probable or possible
64 Class 2A/B carcinogens in humans (IARC, 2014; IARC, 2010).

65 One of the most difficult challenges for risk assessment is the evaluation of health
66 hazards from exposure to environmental chemical mixtures. Currently, significant data gaps
67 exist for understanding carcinogenicity of PAH mixtures and complex environmental mixtures
68 containing PAHs. Further, little is known about the mechanisms of tumorigenesis for PAH
69 mixtures. Current assessment of cancer risk for PAHs involves testing compounds in the 2-year
70 rodent bioassay, which is not practical for screening large numbers of compounds or mixtures
71 due to expense and time. Therefore, alternative approaches are typically utilized for evaluating
72 the carcinogenic potential of PAHs and PAH-containing mixtures. Currently, the primary
73 method for assessing cancer risk of complex mixtures is the relative potency factor (RPF)

1
2
3 74 approach in which complex mixtures are evaluated based on a subset of individual component
4
5 75 PAHs compared to BaP as a surrogate or reference (EPA, 2010). However, we and others have
6
7
8 76 found this approach inadequate for predicting carcinogenicity of mixtures and certain individual
9
10 77 PAHs, particularly those that function through alternate pathways or exhibit greater promotional
11
12
13 78 capacity compared to BaP (Courter *et al.*, 2008; Siddens *et al.*, 2012).

14
15 79 Significant challenges have also been identified in utilizing such reference based
16
17 80 approaches for estimating risk from exposure to PAHs in air pollution or waste sites. Complex
18
19
20 81 environmental mixtures subjected to weathering and aging processes can contain many different
21
22 82 PAHs, including alkyl-, N-, S- and O- substituted forms, along with other unknown chemicals;
23
24 83 however, only a limited number of unsubstituted PAHs have been characterized for use in RPF
25
26
27 84 calculations. Mixture toxicity for risk assessment is calculated based on select individual
28
29 85 components and assumes additivity through a common mechanism of action for PAHs compared
30
31 86 to BaP as a standard. Therefore, the RPF approach does not take into consideration mechanistic
32
33 87 information about the different pathways, cells and tissues affected by PAHs during initiation
34
35
36 88 and promotion. This approach is also insufficient for predicting carcinogenicity of complex real
37
38
39 89 world environmental mixtures of unknown composition.

40
41 90 In this study, we propose an innovative model for determining carcinogenic risk of PAH
42
43 91 mixtures using mechanistic approaches. We hypothesize that a chemical bioactivity profile
44
45
46 92 measured after short term exposure to individual and mixture PAHs from global transcriptional
47
48 93 profiling can be used to discriminate future carcinogenic potential based on important
49
50 94 mechanistic differences among exposures. The bioactivity profile acts as a unique fingerprint for
51
52
53 95 genes and pathways activated by chemicals and mixtures post-exposure and can be used for
54
55 96 predicting long-term consequences such as cancer outcome. An important aspect of the
56
57
58
59
60

1
2
3 97 bioactivity profile is that the gene signatures are linked to chemical mechanism of action and can
4
5 98 also provide insight into alternate mechanisms of PAH carcinogenesis and related mechanisms
6
7
8 99 for complex mixtures. Based on preliminary data, we demonstrate that long term cancer
9
10 100 outcome for PAHs and mixtures can be predicted from high-content genomic evaluation of
11
12 101 bioactivity after short term exposure.
13
14

15 102

17 103 **Materials and Methods**

19 104

21 105 *Chemicals*

23
24 106 BaP and DBC were handled in accordance with National Cancer Institute Guidelines. All
25
26 107 pure PAHs and mixtures were prepared under UV depleted light as described in Siddens *et al.*
27
28 108 (2012). The PAHs and environmental PAH mixtures utilized for initiation of skin carcinogenesis
29
30 109 in animal models are summarized in Table 1. PAH mixture 1 (Mix 1) consisted of 5 mg/ml
31
32 110 diesel particulate exhaust (DPE) in vehicle (toluene containing 5% DMSO). PAH mixture 2
33
34 111 (Mix 2) consisted of 5 mg/ml each DPE and coal tar extract (CTE) in vehicle. PAH mixture 3
35
36 112 (Mix 3) consisted of 5 mg/ml DPE, 5 mg/ml CTE and 10 mg/ml cigarette smoke condensate
37
38 113 (CSC).
39
40
41
42
43
44

45 114

46 115 *Animal studies and tumor analysis*

47
48 116 FVB/N mice were exposed to PAHs or PAH mixtures following a two-stage tumor-
49
50 117 promotion protocol in skin. All procedures were conducted according to National Institutes of
51
52 118 Health guidelines and were approved by the Oregon State University Institutional Animal Care
53
54 119 and Use Committee. Six- week-old, female FVB/N inbred mice obtained from the NCI-
55
56
57
58
59
60

1
2
3 120 Fredrick's Animal Production Program (Frederick, MD) were fed AIN93-G pellets (Research
4
5 121 Diets, Inc., New Brunswick, NJ) throughout the experiment. At 7.5 weeks of age, mice (groups
6
7 122 of 36) were initiated with PAH treatments (summarized in Table 1) by application to shaved skin
8
9 123 in 200 μ l toluene vehicle. Animals for microarray analysis (N=4 or 5 per treatment) were
10
11 124 sacrificed 12 h after treatment and skin was collected for RNA isolation. Two weeks post-
12
13 125 initiation, a 25-week promotion regimen was begun with remaining animals, treating animals
14
15 126 twice weekly with 6.5 nmol 12-O-tetradecanoylphorbol-13-acetate (TPA) in 200 μ l acetone.
16
17 127 Mice were observed and tumor incidence recorded weekly throughout the 25-week promotion
18
19 128 interval. Following promotion, all animals were euthanized and necropsied. Tumors were
20
21 129 removed, fixed in formalin and prepared for histopathology of hematoxylin and eosin-stained
22
23 130 sections to determine stage of progression. Tumor incidence was measured as the percent
24
25 131 incidence for each treatment based on tumor type. Statistical significance among the treatment
26
27 132 groups was calculated by ANOVA with Newman-Keuls multiple testing correction.
28
29
30
31
32
33

34 133

35

36 134 *Microarrays and Gene expression analysis*

37

38
39 135 Individual mouse dermal samples were analyzed by Agilent microarray after initiation
40
41 136 with PAHs (N=4 biological replicates, Table 1) or toluene control (N=5 biological replicates).
42
43 137 RNA was isolated from flash frozen skin samples in Trizol Reagent (Life Technologies,
44
45 138 Carlsbad, CA) followed by clean-up with Qiagen RNeasy mini prep kit (Valencia, CA)
46
47 139 according to manufacturer protocols. RNA quality and quantity were assessed by Agilent
48
49 140 Bioanalyzer (Santa Clara, CA) and Nanodrop spectrophotometry (Thermo Fisher Scientific,
50
51 141 Waltham, MA) analysis, respectively. Samples with $A_{260/280}$ ratios of 1.9-2.2 and RNA integrity
52
53 142 values 6.5 or greater were selected for microarray analysis. For microarrays, RNA was labeled
54
55
56
57
58
59
60

1
2
3 143 with Agilent's 2 color Quickamp kit for hybridization to the Agilent 8 X 60K mouse array. Raw
4
5 144 intensity data were quantile normalized by RMA summarization (Bolstad *et al.*, 2003) and
6
7
8 145 subject to pairwise analysis of variance (Kerr *et al.*, 2000) with Tukey's post hoc test and 5%
9
10 146 false discovery rate calculation (Benjamini Y, 1995).

11
12
13 147

14
15 148 *Bioinformatics*

16
17 149 Unsupervised hierarchical clustering of microarray data was performed using Euclidean
18
19 150 distance metric and centroid linkage clustering to group gene expression patterns by similarity.
20
21 151 The clustering algorithms, heat map visualizations and centroid calculations were performed
22
23 152 with Multi-Experiment Viewer (Saeed *et al.*, 2003) software based on Log₂ expression ratio
24
25 153 values. Functional enrichment analysis was performed in MetaCore (GeneGO, Thomson
26
27 154 Reuters) based on mappings of the significant ($p < 0.05$) genes in each treatment group onto built-
28
29 155 in functional network processes and Gene Ontology biological process categories. Analyses
30
31 156 were performed for each database independently. Metacore's knowledgebase, which is derived
32
33 157 through manual annotation and curation from the literature, was used for the biological network
34
35 158 processes. Statistical significance for enrichment was calculated using a hypergeometric
36
37 159 distribution, where the p-value represents the probability of a particular mapping arising by
38
39 160 chance for experimental data compared to the background, which included all genes on the
40
41 161 Agilent platform (Nikolsky *et al.*, 2009). All processes included more than 15 genes. Gene
42
43 162 Ontology biological processes were further filtered to include only the top 10 most significant
44
45 163 ($p < 5E-7$) processes for each treatment group that were categorized greater than level 2 in the
46
47 164 gene ontology tree to reduce redundancy. To identify major transcriptional regulators of gene
48
49 165 expression by PAHs, the Statistical Interactome tool was used in MetaCore to measure the
50
51
52
53
54
55
56
57
58
59
60

1
2
3 166 interconnectedness of genes in the experimental dataset relative to all known interactions in the
4
5
6 167 background dataset. Statistical significance of over-connected interactions was also calculated
7
8 168 using a hypergeometric distribution. Networks were constructed in MetaCore for experimental
9
10 169 data using an algorithm that identifies the shortest path to directly connect nodes in the dataset to
11
12 170 transcription factors. Network visualizations were created in Cytoscape (Shannon *et al.*, 2003)
13
14
15 171 utilizing the spring embedded layout. PAH treatments were classified based on tumor outcome
16
17 172 with Visual Integration for Bayesian Evaluation (VIBE) v2.0 (Beagley *et al.*, 2010) in which
18
19
20 173 Bayesian integration of significantly enriched ($p < 0.05$) pathways was performed using K-nearest
21
22 174 neighbors statistical learning algorithm (Atiya, 2005) with leave-one-out cross validation. VIBE
23
24 175 performs Bayesian integration of the experimental datasets (i.e. pathways) and provides a
25
26
27 176 classification accuracy based on the integrated probability model (Webb-Robertson *et al.*, 2009).
28

29 177

30 31 32 178 **Results**

33
34 179

35 36 180 *Classification of PAH treatments based on tumor outcome*

37
38
39 181 PAHs and environmental PAH mixtures were classified into low, moderate or high
40
41 182 categories based on their ability to induce tumorigenesis following a two-stage
42
43 183 initiation/promotion skin tumor protocol. Classification was based on statistical evaluation of
44
45
46 184 tumor incidence calculated as the percent incidence per tumor type, which was determined by
47
48 185 histology from the progression from hyperplasia to papilloma, carcinoma *in situ* or squamous
49
50 186 cell carcinoma. Overall, exposure of FVB/N mice to BaP, DBC or 1 of 3 environmental PAH
51
52
53 187 mixtures resulted in treatment-specific tumor incidence profiles; although the relative amounts of
54
55 188 each tumor type was similar across all PAH treatments (Figure 1A). The percent incidence of
56
57
58
59
60

1
2
3 189 papillomas was greatest for all PAHs and PAH mixtures, while carcinoma *in situ* was the least
4
5 190 prevalent tumor type. In animals initiated with vehicle control or Mixture 1, only one papilloma
6
7
8 191 was detected resulting in 3% tumor incidence for each group. Tumor incidence was highest after
9
10 192 initiation with DBC ($p < 0.001$ compared to control), ranging from 50-90% depending on tumor
11
12 193 type. Tumor incidence was similar for BaP, Mix 2 and Mix 3, all of which were significant from
13
14 194 controls ($p < 0.05$) and were not significantly different from each other. Actual percent tumor
15
16 195 incidence, number of animals per treatment group and individual p-values for each tumor type
17
18 196 are provided in Supplemental Data S1. The carcinogenic potential for each PAH treatment was
19
20 197 ranked as DBC >> BaP = Mix 2 = Mix 3 > Mix 1 = Control based on statistical evaluation of tumor
21
22 198 incidence, which was consistent with that previously reported for time until tumor event and
23
24 199 tumor multiplicity for these treatments in mouse skin (Siddens *et al.*, 2012). Based on this
25
26 200 ranking, PAH treatments were categorized as having low (Mix 1), moderate (BaP, Mix 2, Mix 3)
27
28 201 or high (DBC) carcinogenic potential (Figure 1B) for evaluation of mechanisms driving PAH-
29
30 202 mediated carcinogenesis in skin.
31
32
33
34
35

36 203 Overall tumor incidence did not correlate with relative potency calculated based on BaP
37
38 204 equivalency (BaP_{eq}) in Siddens *et al* (2012) in which mixture RPFs are determined using
39
40 205 reported RPFs (EPA, 2010) for known components. Figure 2A shows correlation of actual
41
42 206 tumor incidence (black circles, $r^2 = 0.09$, $R = 0.5$, $p = 0.45$) compared to predicted tumor incidence
43
44 207 from RPFs by Spearman rank. RPF calculations underestimated carcinogenicity of DBC and the
45
46 208 coal-tar containing mixtures (Mix 2 and 3). Induction of Cyp1a1 gene expression measured by
47
48 209 microarray at 12 h post-initiation also correlated very poorly with tumor incidence by treatment
49
50 210 group ($r^2 = 0.004$, $R = -0.30$, $p = 0.68$). Further, DNA adduct formation measured previously in skin
51
52 211 post-initiation (Siddens *et al.*, 2012) did not significantly correlate with tumor incidence
53
54
55
56
57
58
59
60

1
2
3 212 ($r^2=0.14$, $R=0.70$, $p=0.68$) as shown in Figure 2B. DNA adducts were more accurately predicted
4
5 213 by RPFs than tumor incidence (Figure 2C), particularly for DBC treatment. Actual adduct
6
7 214 formation correlated with calculated BaP_{eq} (Spearman 0.90, $p=0.083$; linear regression $r^2=0.95$,
8
9 215 $p=0.005$).

216

217 *PAHs and PAH mixtures have unique gene signatures post-initiation*

17 218 Global gene expression was evaluated in mouse skin by microarray 12 h post-initiation
18
19 219 with BaP, DBC and three environmental PAH mixtures in order to identify gene signatures
20
21 220 during initiation associated with PAH-induced skin carcinogenesis. Overall, 922 genes were
22
23 221 differentially expressed ($p<0.05$) in skin after treatment with any PAH or PAH mixture
24
25 222 compared to vehicle control; including 137, 246, 97, 428 and 521 genes for BaP, DBC, Mix 1,
26
27 223 Mix 2 and Mix 3, respectively (Supplemental Data S2). Comparison of significant genes among
28
29 224 treatments are visualized as a 5-way venn diagram in Supplemental Data S2. Raw and
30
31 225 normalized Agilent data files are available online at
32
33 226 <http://www.ncbi.nlm.nih.gov/geo/query/acc.cgi?acc=GSE39455>. Microarray results were
34
35 227 confirmed using RT-qPCR on a subset of six genes with decreased, increased, and no significant
36
37 228 change in expression levels relative to control (Larkin *et al.*, 2013). Unsupervised bidirectional
38
39 229 hierarchical clustering of all differentially expressed genes resulted in distinct clustering of
40
41 230 biological replicates based on treatment group with clear separation between the individual PAH
42
43 231 exposures (BaP and DBC) and the environmental mixtures (Figure 2D). Gene signatures did not
44
45 232 cluster based on tumor outcome suggesting they were indicative of treatment-specific responses
46
47 233 in skin that were not necessarily contributing to tumorigenesis. This is further supported by the
48
49 234 fact that the total number of genes differentially regulated by each treatment group did not
50
51
52
53
54
55
56
57
58
59
60

1
2
3 235 correlate with overall tumor incidence (Spearman $R=0.3$, $p=0.68$) and linear regression of these
4
5 236 endpoints was not significant from zero ($r^2=0.22$, $p=0.43$). In particular, the environmental PAH
6
7
8 237 mixtures containing coal tar extract (Mix 2 and Mix 3) altered the largest number of transcripts
9
10 238 in skin post-initiation; although, did not result in the highest incidence of skin tumors. Instead,
11
12 239 DBC treatment resulted in the highest tumor incidence while only causing moderate gene
13
14 240 expression in skin post-initiation. Based on the strong similarity in both the gene expression
15
16 241 patterns and overall tumor incidence by Mix 2 and Mix3, it is apparent their response was either
17
18 242 driven by the coal tar extract alone or by the cumulative effect of diesel exhaust and coal tar
19
20 243 extract present in the mixtures with minimal impact from the addition of cigarette smoke
21
22 244 condensate to Mix 3.
23
24
25

26
27 245 Even though the overall transcriptional response was unrelated to tumor outcome, there
28
29 246 were clusters of genes with gene expression patterns similar to the tumor profiles for these PAHs
30
31 247 suggesting that a subset of the transcriptional data may be predictive of tumor outcome. The
32
33 248 enlarged heatmap in Figure 2D shows one example cluster of genes that are highly differentially
34
35 249 expressed for BaP, Mix 2 and Mix 3 with a distinct pattern of response from DBC indicating that
36
37 250 this particular gene cluster may be relevant for initiation of PAH-induced skin cancer. Genes in
38
39 251 this cluster included several phase I and II metabolizing enzymes known to be involved in
40
41 252 metabolism of PAHs, including *Gsta1*, *Gsta2*, *Gsta3*, *Gpx2*, *Cyp1a1*, *Cyp1b1* and *Nqo1*.
42
43 253 Therefore, in order to identify the subset of gene changes during initiation that may be predictive
44
45 254 of tumor outcome, we used the full gene expression dataset to systematically model gene
46
47 255 changes driving carcinogenesis.
48
49
50
51
52

53 256

54
55 257 *Pathway-based classification of tumor outcome*
56
57
58
59
60

1
2
3 258 We hypothesized that PAH-induced gene regulation from biological pathways most
4
5
6 259 closely associated with induction of carcinogenesis could be predictive of tumor outcome after
7
8 260 exposure. Further, we hypothesized that the mechanism-based gene signatures associated with
9
10 261 these pathways could be used to classify potential carcinogens based on their carcinogenic
11
12 262 potential. The biological processes that met significance criteria (as described in the Methods)
13
14
15 263 for Gene Ontology and Metacore processes are shown in Figure 3 as a heatmap in which the
16
17 264 most significant functions for each treatment are colored blue and the least significant are
18
19
20 265 colored black. Actual enrichment p-values are provided in Supplemental Data S3. Overall, the
21
22 266 functions enriched in skin after initiation with Mix 2 and 3 are very similar to each other and
23
24 267 mostly unique from the functions enriched for the individual PAH treatments of BaP and DBC.
25
26
27 268 The most significant processes for mixtures 2 and 3 include those associated with cell cycle,
28
29 269 mitosis and response to xenobiotic or DNA damage stimulus. Fewer biological processes are
30
31 270 significant post-initiation with BaP and include those associated with xenobiotic metabolism and
32
33
34 271 response to chemical stimulus and oxidative stress. There is little overlap in the processes
35
36 272 significant between BaP and DBC and those enriched post-initiation with DBC include cell
37
38 273 cycle, apoptosis, interphase of mitosis and ubiquitin-dependent catabolic processes. While
39
40 274 significant enrichment of these functions post-initiation by PAHs provides a basis for
41
42
43 275 understanding their individual mechanisms of action, they do not necessarily indicate which
44
45
46 276 pathways are linked to PAH carcinogenic response. In fact, Mix 1, which did not induce skin
47
48 277 tumors, significantly altered several pathways in common with Mix 2/3 associated with DNA-
49
50 278 protein complex assembly or nucleosome assembly, suggesting that these processes are not
51
52
53 279 associated with carcinogenic outcome (Figure 3).
54
55
56
57
58
59
60

1
2
3 280 Therefore, in order to systematically filter the significant pathway list in Figure 3 to only
4
5 281 those associated with skin carcinogenesis, the microarray transcripts from enriched Gene
6
7
8 282 Ontology and MetaCore processes were evaluated for their ability to classify the PAH treatment
9
10 283 groups based on tumor outcome utilizing a Bayesian integration framework. This approach
11
12 284 evaluates the ability of the genes differentially expressed in each pathway to classify the PAH
13
14 285 exposures based on tumor outcome (low, moderate or high) utilizing the k-nearest neighbors
15
16 286 statistical learning algorithm to build likelihood probability models for each pathway. A
17
18 287 classification accuracy was calculated for each pathway based on the number of correctly
19
20 288 classified samples compared to the total number of samples. In this case, each sample is an
21
22 289 individual animal or biological replicate in the study. Since it is likely that multiple pathways
23
24 290 are contributing to the carcinogenic potential of the different PAHs and environmental PAH
25
26 291 mixtures, we integrated the posterior probabilities of each pathway utilizing a Bayesian approach
27
28 292 to further identify the subset of pathways that result in the highest classification accuracy when
29
30 293 integrated together. As shown in Figure 4A, four pathways have high individual classification
31
32 294 accuracies, ranging 0.80 – 0.90, including 1) Response to DNA damage stimulus, 2) Regulation
33
34 295 of apoptosis, 3) Cellular response to chemical stimulus and 4) Interferon gamma signaling.
35
36 296 When integrated together, the overall classification accuracy improves and the 4 pathways above
37
38 297 predict tumor outcome with 100% classification accuracy indicating their importance for the
39
40 298 carcinogenic potential of PAHs during initiation.

41
42 299 A total of 172 genes are represented in the pathways from Figure 4A and were
43
44 300 differentially expressed in skin post-initiation by PAHs. The list of genes from the predictive
45
46 301 pathways are provided in Supplemental Data S4. Principal components analysis (PCA) on this
47
48 302 gene set allows for visualization of how these particular genes, reduced from 55K on the Agilent
49
50
51
52
53
54
55
56
57
58
59
60

1
2
3 303 array, may be driving tumor response after PAH initiation (Figure 4B). Clustering of the
4
5 304 samples by PCA clearly distinguishes the samples based on carcinogenic potential, such that the
6
7
8 305 control and Mix 1 samples group together (Low), the Mix 2, Mix 3 and BaP samples group
9
10 306 together (Moderate) and the DBC samples group together (High). In addition to predicting
11
12 307 carcinogenesis of the PAHs tested in this study, our data suggest that this approach could also be
13
14 308 used to predict carcinogenic potential of unknown PAHs or environmental PAH mixtures in skin
15
16 309 based on short-term exposure assessment with additional evaluation and validation.
17
18
19
20 310

21
22 311 *Distinct transcriptional regulators driving PAH-mediated gene expression in predictive*
23
24 312 *pathways*

25
26
27 313 To understand how the pathways predictive of PAH carcinogenesis are regulated in skin
28
29 314 during initiation, we performed transcription factor enrichment analysis on the significant genes
30
31 315 differentially expressed (out of 172 genes) by each PAH treatment within the predictive
32
33 316 pathways. Table 2 lists the transcription factors for each treatment that are significantly ($p < 0.05$)
34
35 317 over-connected (i.e. transcription factors with a significant number of downstream target genes
36
37 318 that are differentially expressed in the gene list compared to that calculated by chance). The
38
39 319 most significant transcription factors regulating gene expression after treatment with BaP, Mix 2
40
41 320 and Mix 3 include Arnt, Nrf2 and Sp1. In contrast, DBC-treated genes were most significantly
42
43 321 regulated by Myc and p53 resulting in a relatively higher tumor response. These results indicate
44
45 322 that there are distinct mechanisms regulating gene expression post-initiation leading to moderate
46
47 323 and high levels of skin tumors after PAH exposure. The gene regulatory networks associated
48
49 324 with each treatment are shown in Figure 5. Through investigation of the sub-networks for BaP
50
51 325 and the PAH mixtures 2 and 3, it is apparent that even though they regulate transcription through
52
53
54
55
56
57
58
59
60

1
2
3 326 the same transcription factors, there are many differentially expressed genes that are unique to
4
5 327 each treatment group. The genes that are regulated in common between BaP and the mixtures
6
7
8 328 primarily include Phase I and Phase II enzymes important for the activation and metabolism of
9
10 329 PAHs. Most of these genes were not significant after treatment with Mix 1 and none were
11
12
13 330 significant post-initiation with DBC. Overall, however, the treatments associated with a
14
15 331 moderate tumor response are more similar at the pathway level than at the gene level suggesting
16
17 332 that gene regulation within pathways make better predictors of tumor outcome than a suite of
18
19
20 333 individual gene biomarkers. Transcriptional regulation of genes associated with a high tumor
21
22 334 outcome were mostly unique to DBC treatment (Figure 5).
23
24
25 335

26 336 **Discussion**

27 337
28
29
30
31 338 Environmental mixtures containing PAH chemicals are of continued and emerging
32
33 339 concern because of the existing significant data gaps for understanding their carcinogenic
34
35 340 potential and their modes of action as carcinogens. Certain individual PAHs, including BaP and
36
37 341 DBC used in our study, are known to produce tumors in mouse skin, lung, liver and breast and
38
39 342 were recently elevated to Class 1 known and Class 2A probable human carcinogens, respectively
40
41 343 (IARC, 2010). However, most human PAH exposures result from chemical mixtures of multiple
42
43 344 PAHs. Current risk assessment of PAHs primarily relies on the reference-based approach of
44
45 345 applying RPFs compared to BaP equivalents for estimating carcinogenicity, which assumes a
46
47 346 common mode of action for PAH-induced tumors. We have previously identified tumor profiles
48
49 347 for several individual and mixture PAHs that did not correlate with calculated RPF values or
50
51 348 with formation of DNA adducts in the two-stage mouse skin tumor model ((Siddens *et al.*, 2012),
52
53
54
55
56
57
58
59
60

1
2
3 349 Figure 2A-B). For the most part, calculated RPFs based on BaP_{eq} underestimated potency in
4
5
6 350 skin. In particular, DBC, which has a reported RPF of 30 was found to be over 100-fold more
7
8 351 potent than BaP in our study. Also, the PAH mixtures containing coal tar extract (Mix 2 and 3)
9
10 352 induced tumors with similar incidence, multiplicity and latency to BaP despite calculated BaP_{eqs}
11
12 353 of 0.34 and 0.47, respectively, which suggested much lower potency. We also found that the
13
14 354 addition of cigarette smoke condensate in Mix 3 did not produce an elevated tumor response
15
16
17 355 above Mix 2 as was predicted based on the relative BaP_{eq}. These data support the idea that RPFs
18
19
20 356 do not accurately reflect carcinogenicity of certain individual PAHs or PAH mixtures, which
21
22 357 likely involve more complex interactions among PAHs than can be predicted based on BaP_{eq}
23
24 358 additivity resulting in either an under or over estimation of carcinogenic potential. We therefore
25
26
27 359 decided to evaluate the mechanisms for initiation of skin tumors by BaP and DBC using gene
28
29 360 expression profiling and determine if reference mixtures reflect similar or distinct mode of action
30
31
32 361 compared to the individual PAHs.

33 34 362 35 36 363 *Pathway-based classification of carcinogenicity*

37
38 364 In this study, we propose a method for predicting potency of PAH chemicals and
39
40
41 365 environmental PAH mixtures based on a bioactivity profile derived from global transcriptional
42
43 366 analysis short-term post-exposure. Using our initial dataset in mouse skin as proof-of-concept,
44
45
46 367 we provide evidence that a subset of genes and pathways are capable of classifying PAHs and
47
48 368 mixtures by carcinogenic potency. This approach does not require *a priori* knowledge of
49
50 369 individual components in mixtures nor does it assume a common mechanism of action for all
51
52
53 370 PAHs and mixtures. Instead, we propose that chemical-specific signaling after exposure
54
55 371 provides a unique signature or bioactivity profile for each PAH/mixture that is reflective of its
56
57
58
59
60

1
2
3 372 mode of action and can be used to discriminate carcinogenic potency. Our current data suggests
4
5 373 that gene expression within four pathways related to DNA damage, apoptosis, response to
6
7
8 374 chemical stimulus and interferon gamma signaling were most important for describing variance
9
10 375 in our skin model system associated with carcinogenesis of PAHs. When all four pathways were
11
12 376 integrated together using a Bayesian framework, samples were classified correctly by potency
13
14
15 377 nearly 100% of the time. Therefore, we provide evidence that short-term bioactivity profiles for
16
17 378 a subset of pathways can be used to predict carcinogenic potential of unknown samples and
18
19
20 379 mixtures.

21
22 380 The use of high-throughput data in toxicogenomics for identifying gene signatures and
23
24 381 biomarkers associated with toxicity and disease phenotype is increasingly common; however, the
25
26
27 382 application of systems approaches to risk assessment is still in the early stages of evaluation
28
29 383 (Lesko *et al.*, 2013). We believe that utilization of these approaches for complex environmental
30
31 384 mixtures is an excellent case study for risk assessment due to the significant lack of knowledge
32
33
34 385 regarding mixture toxicity and constituency. Similar genomic-based models have successfully
35
36 386 been applied to individual chemicals after short-term exposure to identify modes of action for
37
38
39 387 distinguishing hepatocarcinogens from non-carcinogens from *in vivo* rat and *in vitro* human
40
41 388 models (Gusenleitner *et al.*, 2014; Song *et al.*, 2012). In particular, Gusenleitner *et al.* (2014),
42
43 389 noted the tissue-specific responses observed when modeling carcinogenicity of a broad range of
44
45
46 390 chemicals from short-term genomic responses. While our study only utilizes data from skin, it
47
48 391 also more directly focuses on modeling responses to PAHs and PAH-containing mixtures. We
49
50 392 believe that the results of this more focused dataset could be extended to other tissues and
51
52
53 393 exposure routes. Transcriptional signatures have been used successfully to evaluate responses to
54
55 394 complex and binary mixtures in multiple tissues and in a summary of comparative gene
56
57
58
59
60

1
2
3 395 expression analyses induced by various complex PAH-containing mixtures *in vitro* and *in vivo*,
4
5 396 several consensus pathways were identified associated with oxidative stress response,
6
7
8 397 metabolism and immune response that overlap with our predicted dataset (Huang, 2013; Sen *et*
9
10 398 *al.*, 2007). For each functional group, different genes were altered by the extracts supporting our
11
12 399 finding that regulation within these pathways could be used to discriminate toxicity amongst
13
14 400 complex PAH mixtures. Other studies that have modeled non-additive effects of polycyclic
15
16 401 aromatic compounds in mixtures on hepatotoxicity utilizing differential gene expression report
17
18 402 the strong correlation of gene response with other toxicity endpoints *in vivo*, including
19
20 403 histopathology, gross physiology (e.g. liver weight) and hepatic lipid composition (Kopec *et al.*,
21
22 404 2010; Kopec *et al.*, 2011). These studies show the benefits of using gene expression to evaluate
23
24 405 quantitative differences in mixture toxicity compared to individual components.
25
26
27
28
29
30

31 407 *Use of bioactivity profiles for understanding toxicity mechanisms*

32
33
34 408 The bioactivity profiles identified through our classification approach reflect processes
35
36 409 contributing towards PAH chemical mode of action. Network and transcription factor analysis
37
38 410 of the predictive gene clusters further resulted in identification of the upstream transcriptional
39
40 411 regulators associated with skin cancer. Overall, we observed distinct gene expression profiles
41
42 412 linked to tumor outcome for PAHs and PAH mixtures. DBC treatment, which had the greatest
43
44 413 tumor response, uniquely altered genes associated with cell cycle and DNA damage pathways
45
46 414 mediated by p53 and c-Myc; while BaP and PAH mixtures containing coal tar were less
47
48 415 carcinogenic and altered genes associated with metabolic and stress response pathways mediated
49
50 416 by Arnt, Nrf2 and Sp1. The latter response is more typical of metabolic changes and induction
51
52
53 417 in Phase I and II enzymes associated with exposure to PAHs, such as BaP, as shown in purple in
54
55
56
57
58
59
60

1
2
3 418 the integrative network in Figure 5. The magnitude of gene expression for these enzymes was
4
5
6 419 used, in part, to distinguish and classify PAHs and PAH mixtures based on carcinogenic
7
8 420 potential, including the non-carcinogenic Mix 1 containing only the diesel exhaust particulate
9
10 421 SRM. However, gene expression for other unique pathways was prognostic for DBC, which
11
12 422 appears to function through alternate modes of action. The highly distinct mechanisms regulated
13
14
15 423 by different PAHs short-term after exposure suggest activation of unique stress response
16
17 424 pathways instead of a common mechanism of action for all PAHs.

19
20 425 These data help to support a whole mixture approach to risk assessment over a
21
22 426 component-based approach, which requires chemical characterization of complex mixtures and
23
24 427 assumes common mechanisms of actions for all PAHs. Whole mixture and comparative
25
26
27 428 potency approaches have been proposed by the EPA and others (EPA, 2010; Jarvis *et al.*, 2014)
28
29 429 as more appropriate for complex mixtures when chemical characterization is not possible. These
30
31 430 approaches are also better suited for evaluating complex chemical interactions within mixtures
32
33
34 431 because they do not rely on predicting the effects of interactions (e.g. additive versus inhibitory)
35
36 432 based on knowledge of the individual components. As we observed in our study in the example
37
38 433 of Mix 3, an additive response cannot be assumed. The addition of cigarette smoke condensate
39
40 434 to Mix 3 did not result in elevated tumor response as expected by RPF calculations. Others have
41
42
43 435 reported similar lack of additive response with PAH mixtures on tumor outcome and suggested
44
45 436 antagonistic effects on metabolizing enzymes as the cause (Courter *et al.*, 2008). Instead, whole
46
47 437 mixture assessment using mixture assessment factors (as discussed by (Backhaus and Faust,
48
49 438 2010; Jarvis *et al.*, 2014)) compares the effects of whole mixtures based on a molecular
50
51 439 biological endpoint, such as activation of DNA damage signaling. We propose that instead of
52
53
54 440 focusing on a single endpoint, the whole mixture approach to risk assessment could be based on
55
56
57
58
59
60

1
2
3 441 bioactivity profiles of predicted gene sets. Integration across several biological processes using a
4
5 442 Bayesian approach improves overall classification accuracy. This approach could potentially be
6
7
8 443 used to determine the quantitative relationships between modes of action so that better potency
9
10 444 factors could be calculated for the purpose of evaluating risk among mixtures from various
11
12 445 sources. The EPA Framework for use of genomics data provides that toxicogenomics data may
13
14 446 be useful in a weight-of-evidence approach for assessing risk (Dix *et al.*, 2006). As such, this
15
16 447 pathway-driven approach was successfully utilized to distinguish early regulatory events during
17
18 448 initiation linked to tumor outcome and shows the potential of using short-term initiation studies
19
20 449 for prediction of carcinogenesis by environmental PAH mixtures. These data provide a ‘source-
21
22 450 to-outcome’ model that could be used to predict PAH interactions during tumorigenesis and
23
24 451 provide mode-of-action based risk assessment of environmental PAH mixtures.
25
26
27
28
29
30

31 452

32 453 **Supplementary Data**

33
34 454 Supplementary data are available online at <http://toxsci.oxfordjournals.org/>.

35
36 455 **Supplemental Data S1.** Percent tumor incidence, number of animals per treatment group and
37
38 456 individual p-values for each tumor type.

39
40 457 **Supplemental Data S2.** The list of significant genes for each treatment and 5-way venn
41
42 458 comparison of significant genes among treatment groups.

43
44 459 **Supplemental Data S3.** The list of significantly enriched Metacore processes and GO biological
45
46 460 process terms.

47
48 461 **Supplemental Data S4.** The list of genes from the predictive pathways used for classification.
49
50
51
52

53 462

54 55 463 **Funding**

1
2
3 464 This work was supported by the National Institute of Environmental Health Sciences grants P42
4
5 465 ES016465, ARRA Supplement to Promote Diversity in Health Research P42 ES016465-S1 and
6
7
8 466 P01 CA90890.
9

10 467

11
12
13 468 **Acknowledgements**

14
15 469 The authors thank Dr. Hollie Swanson, from the University of Kentucky, for providing cigarette
16
17 470 smoke condensate and the Laboratory Animal Resources Center at Oregon State University for
18
19 471 help with the animal studies. We also acknowledge Dr. Chris Bradfield and Bradley Stewart at
20
21 472 the University of Wisconsin EDGE3 Core Facility for processing of microarrays. We further
22
23 473 thank Dr. Derek Janszen for statistical analysis of tumor incidence by type. Pacific Northwest
24
25 474 National Laboratory is a multi-program national laboratory operated by Battelle Memorial
26
27 475 Institute for the DOE under contract number DE-AC05-76RLO1830.
28
29
30
31

32 476

33
34 477 **References**

35
36 478 Atiya, A. F. (2005). Estimating the posterior probabilities using the k-nearest neighbor rule.
37
38
39 479 *Neural computation* 17(3), 731-40.
40
41 480 Backhaus, T., and Faust, M. (2010). Hazard and risk assessment of chemical mixtures under
42
43 481 REACH: State of the art, gaps and options for improvement. *Swedish Chemicals Agency*
44
45 482 Bromma, Sweden, Report PM/3.
46
47
48 483 Beagley, N., Stratton, K. G., and Webb-Robertson, B. J. (2010). VIBE 2.0: visual integration for
49
50 484 bayesian evaluation. *Bioinformatics (Oxford, England)* 26(2), 280-2.
51
52
53
54
55
56
57
58
59
60

- 1
2
3 485 Benjamini Y, H. Y. (1995). Controlling the False Discovery Rate: A Practical and Powerful
4
5
6 486 Approach to Multiple Testing. *Journal of the Royal Statistical Society. Series B*
7
8 487 (*Methodological*) 57(1), 289-300
9
10 488 Bolstad, B. M., Irizarry, R. A., Astrand, M., and Speed, T. P. (2003). A comparison of
11
12 489 normalization methods for high density oligonucleotide array data based on variance and
13
14 490 bias. *Bioinformatics (Oxford, England)* 19(2), 185-93.
15
16
17 491 Courter, L. A., Luch, A., Musafia-Jeknic, T., Arlt, V. M., Fischer, K., Bildfell, R., Pereira, C.,
18
19 492 Phillips, D. H., Poirier, M. C., and Baird, W. M. (2008). The influence of diesel exhaust
20
21 493 on polycyclic aromatic hydrocarbon-induced DNA damage, gene expression, and tumor
22
23 494 initiation in Sencar mice in vivo. *Cancer letters* 265(1), 135-47.
24
25
26 495 Dix, D. J., Gallagher, K., Benson, W. H., Groskinsky, B. L., McClintock, J. T., Dearfield, K. L.,
27
28 496 and Farland, W. H. (2006). A framework for the use of genomics data at the EPA. *Nature*
29
30 497 *biotechnology* 24(9), 1108-11.
31
32
33 498 EPA, U. S. (2010). Development of a relative potency factor (RPF) approach for polycyclic
34
35 499 aromatic hydrocarbon (PAH) mixtures. In (U. S. E. P. Agency, Ed.) Eds.) doi:
36
37 500 EPA/635/R-08/012A, Washington, D.C.
38
39
40 501 Gusenleitner, D., Auerbach, S. S., Melia, T., Gomez, H. F., Sherr, D. H., and Monti, S. (2014).
41
42 502 Genomic models of short-term exposure accurately predict long-term chemical
43
44 503 carcinogenicity and identify putative mechanisms of action. *PloS one* 9(7), e102579.
45
46
47 504 Huang, Y. C. (2013). The role of in vitro gene expression profiling in particulate matter health
48
49 505 research. *Journal of toxicology and environmental health. Part B, Critical reviews* 16(6),
50
51 506 381-94.
52
53
54
55
56
57
58
59
60

- 1
2
3 507 IARC (2010). Some non-heterocyclic polycyclic aromatic hydrocarbons and some related
4
5 508 exposures. *Monographs on the evaluation of carcinogenic risks to humans* 92.
6
7
8 509 IARC (2014). Diesel exhaust and gasoline engine exhausts and some nitroarenes. *IARC*
9
10 510 *Monographs and the Evaluation of Carcinogenic Risks to Humans* 105.
11
12 511 Jarvis, I. W., Dreij, K., Mattsson, A., Jernstrom, B., and Stenius, U. (2014). Interactions between
13
14 512 polycyclic aromatic hydrocarbons in complex mixtures and implications for cancer risk
15
16 513 assessment. *Toxicology* 321, 27-39.
17
18
19
20 514 Kerr, M. K., Martin, M., and Churchill, G. A. (2000). Analysis of variance for gene expression
21
22 515 microarray data. *Journal of computational biology : a journal of computational*
23
24 516 *molecular cell biology* 7(6), 819-37.
25
26
27 517 Kopec, A. K., Burgoon, L. D., Ibrahim-Aibo, D., Burg, A. R., Lee, A. W., Tashiro, C., Potter, D.,
28
29 518 Sharratt, B., Harkema, J. R., Rowlands, J. C., Budinsky, R. A., and Zacharewski, T. R.
30
31 519 (2010). Automated dose-response analysis and comparative toxicogenomic evaluation of
32
33 520 the hepatic effects elicited by TCDD, TCDF, and PCB126 in C57BL/6 mice.
34
35 521 *Toxicological sciences : an official journal of the Society of Toxicology* 118(1), 286-97.
36
37
38 522 Kopec, A. K., D'Souza, M. L., Mets, B. D., Burgoon, L. D., Reese, S. E., Archer, K. J., Potter,
39
40 523 D., Tashiro, C., Sharratt, B., Harkema, J. R., and Zacharewski, T. R. (2011). Non-
41
42 524 additive hepatic gene expression elicited by 2,3,7,8-tetrachlorodibenzo-p-dioxin (TCDD)
43
44 525 and 2,2',4,4',5,5'-hexachlorobiphenyl (PCB153) co-treatment in C57BL/6 mice.
45
46 526 *Toxicology and applied pharmacology* 256(2), 154-67.
47
48
49
50 527 Larkin, A., Siddens, L. K., Krueger, S. K., Tilton, S. C., Waters, K. M., Williams, D. E., and
51
52 528 Baird, W. M. (2013). Application of a fuzzy neural network model in predicting
53
54
55
56
57
58
59
60

- 1
2
3 529 polycyclic aromatic hydrocarbon-mediated perturbations of the Cyp1b1 transcriptional
4
5 530 regulatory network in mouse skin. *Toxicology and applied pharmacology* 267(2), 192-9.
6
7
8 531 Lesko, L. J., Zheng, S., and Schmidt, S. (2013). Systems approaches in risk assessment. *Clinical*
9
10 532 *pharmacology and therapeutics* 93(5), 413-24.
11
12 533 Nikolsky, Y., Kirillov, E., Zuev, R., Rakhmatulin, E., and Nikolskaya, T. (2009). Functional
14
15 534 analysis of OMICs data and small molecule compounds in an integrated "knowledge-
16
17 535 based" platform. *Methods in molecular biology (Clifton, N.J.)* 563, 177-96.
18
19
20 536 Saeed, A. I., Sharov, V., White, J., Li, J., Liang, W., Bhagabati, N., Braisted, J., Klapa, M.,
21
22 537 Currier, T., Thiagarajan, M., Sturn, A., Snuffin, M., Rezantsev, A., Popov, D., Ryltsov,
23
24 538 A., Kostukovich, E., Borisovsky, I., Liu, Z., Vinsavich, A., Trush, V., and Quackenbush,
25
26 539 J. (2003). TM4: a free, open-source system for microarray data management and analysis.
27
28 540 *BioTechniques* 34(2), 374-8.
29
30
31 541 Sen, B., Mahadevan, B., and DeMarini, D. M. (2007). Transcriptional responses to complex
32
33 542 mixtures: a review. *Mutation research* 636(1-3), 144-77.
34
35
36 543 Shannon, P., Markiel, A., Ozier, O., Baliga, N. S., Wang, J. T., Ramage, D., Amin, N.,
37
38 544 Schwikowski, B., and Ideker, T. (2003). Cytoscape: a software environment for
39
40 545 integrated models of biomolecular interaction networks. *Genome research* 13(11), 2498-
41
42 546 504.
43
44
45 547 Siddens, L. K., Larkin, A., Krueger, S. K., Bradfield, C. A., Waters, K. M., Tilton, S. C., Pereira,
46
47 548 C. B., Lohr, C. V., Arlt, V. M., Phillips, D. H., Williams, D. E., and Baird, W. M. (2012).
48
49 549 Polycyclic aromatic hydrocarbons as skin carcinogens: comparison of benzo[a]pyrene,
50
51 550 dibenzo[def,p]chrysene and three environmental mixtures in the FVB/N mouse.
52
53 551 *Toxicology and applied pharmacology* 264(3), 377-86.
54
55
56
57
58
59
60

- 1
2
3 552 Song, M. K., Song, M., Choi, H. S., Kim, Y. J., Park, Y. K., and Ryu, J. C. (2012). Identification
4
5 553 of molecular signatures predicting the carcinogenicity of polycyclic aromatic
6
7
8 554 hydrocarbons (PAHs). *Toxicology letters* 212(1), 18-28.
9
10 555 Webb-Robertson, B. J., McCue, L. A., Beagley, N., McDermott, J. E., Wunschel, D. S., Varnum,
11
12 556 S. M., Hu, J. Z., Isern, N. G., Buchko, G. W., McAteer, K., Pounds, J. G., Skerrett, S. J.,
13
14
15 557 Liggitt, D., and Frevert, C. W. (2009). A Bayesian integration model of high-throughput
16
17 558 proteomics and metabolomics data for improved early detection of microbial infections.
18
19 559 *Pacific Symposium on Biocomputing. Pacific Symposium on Biocomputing* doi, 451-63.
20
21
22
23 560
24
25 561
26
27
28
29
30
31
32
33
34
35
36
37
38
39
40
41
42
43
44
45
46
47
48
49
50
51
52
53
54
55
56
57
58
59
60

1
2
3 562 **Figure Legends**

4
5 563 **Figure 1. Classification of PAH and PAH mixture carcinogenic potential based on tumor**
6
7
8 564 **incidence.** Exposure of female FVB/N mice to PAHs following a two-stage initiation/promotion
9
10 565 skin tumor protocol resulted in (A) tumor incidence profiles of
11
12 566 DBC>>>BaP=Mix2=Mix3>>Mix1=Control, based on statistical significance (***) $p<0.0001$,
13
14
15 567 $*p<0.05$ by One-way ANOVA with Newman-Keuls multiple testing correction). Tumor
16
17 568 incidence was calculated as the percent incidence for each treatment based on tumor type. (B)
18
19 569 Based on this ranking, PAH treatments were categorized as having low, moderate or high
20
21
22 570 carcinogenic potential in mouse skin.

23
24 571
25
26
27 572 **Figure 2. Correlation of traditional endpoints with tumor incidence in mouse skin after**
28
29 573 **exposure to PAHs and PAH mixtures.** (A) Comparison of actual tumor incidence measured in
30
31 574 skin to predicted tumor incidence calculated from BaP equivalency (BaP_{eq}). Actual tumor
32
33 575 incidence did not significantly correlate with calculated RPFs (Spearman $R=0.50$, $p=0.45$; linear
34
35 576 regression $r^2=0.09$, $p=0.62$). (B) Correlation of DNA adduct formation (circles) and expression
36
37 577 of Cyp1a1 transcripts (squares) with tumor incidence by Spearman rank. Linear regression was
38
39 578 not significant from zero ($p>0.43$). (C) Comparison of actual DNA adducts measured in skin by
40
41 579 ³²P-postlabeling (Siddens *et al.*, 2012) to predicted adducts calculated from BaP_{eq}. Actual adduct
42
43 580 formation correlated with calculated RPFs with Spearman $R=0.90$ ($p=0.08$) and linear regression
44
45
46 581 $r^2=0.95$ ($p=0.005$). (D) Global gene expression in mouse skin 12 h post-initiation. Unsupervised
47
48 582 clustering of 922 genes differentially expressed ($p<0.05$, 5% FDR) across all treatments.
49
50
51 583 Enlarged heatmap shows gene cluster of highly differentially expressed genes in BaP, Mix2 and
52
53 584 Mix3 groups. Values are log₂ fold change for all treatments compared with control; red, green,
54
55
56 585 and black represent up-regulated, down-regulated and unchanged genes, respectively.
57
58
59
60

586

587 **Figure 3. Pathways significantly enriched ($p<0.05$) in skin post-initiation by PAH and PAH**

588 **mixtures.** Functional enrichment analysis was performed in MetaCore (GeneGO, Thomson

589 Reuters) based on mappings of the significant ($p<0.05$) genes in each treatment group onto built-

590 in functional network processes and Gene Ontology biological process categories. Statistical

591 significance for enrichment was calculated using a hypergeometric distribution. All processes

592 included more than 15 genes. Gene Ontology biological processes were further filtered to

593 include only the top 10 most significant ($p<5E-7$) processes for each treatment group that were

594 categorized greater than level 2 in the Gene Ontology tree.

595

596 **Figure 4. Classification of PAHs and PAH mixture treatments based on tumor outcome.**

597 (A) Bayesian integration of pathways using k-nearest neighbors statistical learning algorithm

598 with leave-one-out cross validation improves classification accuracy of PAH treatments based on

599 tumor outcome. The color scale for the heat maps indicates accuracy for actual versus predicted

600 classification of treatments into the low, moderate and high tumor categories. Highest

601 classification accuracy (100%) is indicated in red and lowest (0%) in white. The panel on the

602 left-hand side shows classification accuracy for each pathway individually and the panel on the

603 right-hand side shows the classification accuracy for all four pathways integrated. (B) Principal

604 components analysis of the predictive gene set shows separation of treated animals based on

605 tumor outcome.

606

607 **Figure 5. Network analysis of pathways predictive of PAH carcinogenic potential during**

608 **initiation in mouse skin.** Gene networks for predictive pathways are visualized for DBC

609 (green), BaP (blue) and Mix2/3 (red). Transcription factors significantly over-connected

1
2
3 610 ($p < 0.05$) by hypergeometric distribution to downstream gene expression networks were
4
5
6 611 identified for each PAH treatment (Table) and are highlighted (circles) in the network figure. In
7
8 612 particular, DBC displays unique gene expression and regulation compared to BaP and the PAH-
9
10 613 mixtures.
11
12
13
14
15
16
17
18
19
20
21
22
23
24
25
26
27
28
29
30
31
32
33
34
35
36
37
38
39
40
41
42
43
44
45
46
47
48
49
50
51
52
53
54
55
56
57
58
59
60

614 Table 1. PAH treatments

Treatment	Components			
Control	200 μ l toluene			
BaP	200 μ l toluene	400 nM BaP		
DBC	200 μ l toluene	4 nM DBC		
Mix 1	200 μ l toluene	1 mg DPE		
Mix 2	200 μ l toluene	1 mg DPE	1 mg CTE	
Mix 3	200 μ l toluene	1 mg DPE	1 mg CTE	2 mg CSC

615 BaP – Benzo[α]pyrene (100 μ g) (Midwest Research Institute, Kansas City, MO)

616 DBC – Dibenzo[*def,p*]chrysene (1.2 μ g) (Midwest Research Institute, Kansas City, MO)

617 DPE – Diesel particulate extract (SRM 1650b, National Institute of Standards and Technology,

618 Gaithersburg, MD)

619 CTE – Coal tar extract (SRM 1597a, National Institute of Standards and Technology,

620 Gaithersburg, MD)

621 CSC – Cigarette smoke condensate (provided by Hollie Swanson, University of Kentucky)

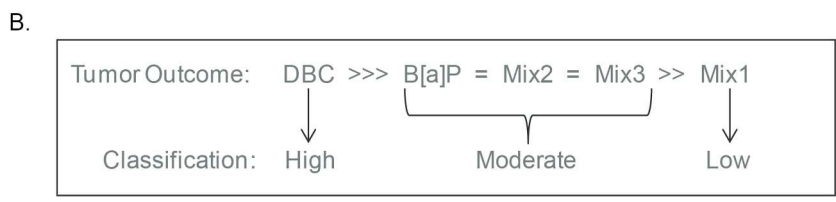
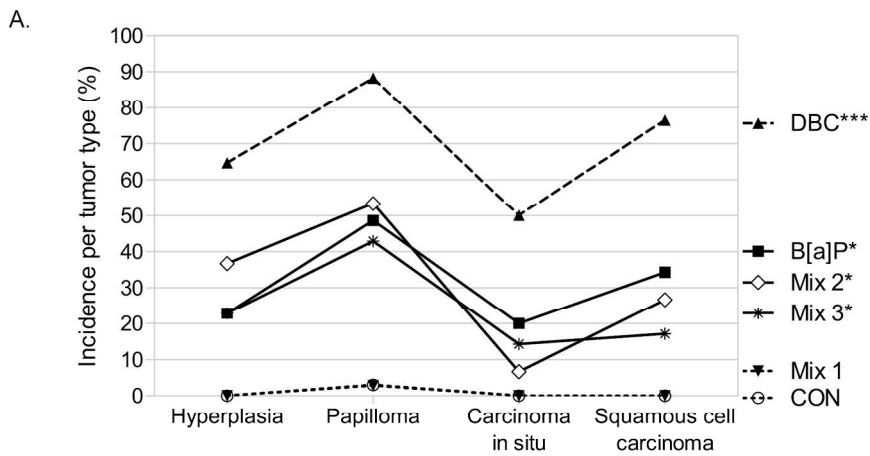
622 Table 2. Transcription factor analysis

Transcription Factor	BaP	DBC	Mix 1	Mix 2	Mix 3
ARNT	***		**	***	****
NRF2	****			****	****
SP1	****	*		****	****
P53		****			
C-MYC		****			

623 **** $p < 0.00001$, *** $p < 0.0001$, ** $p < 0.001$, * $p < 0.05$

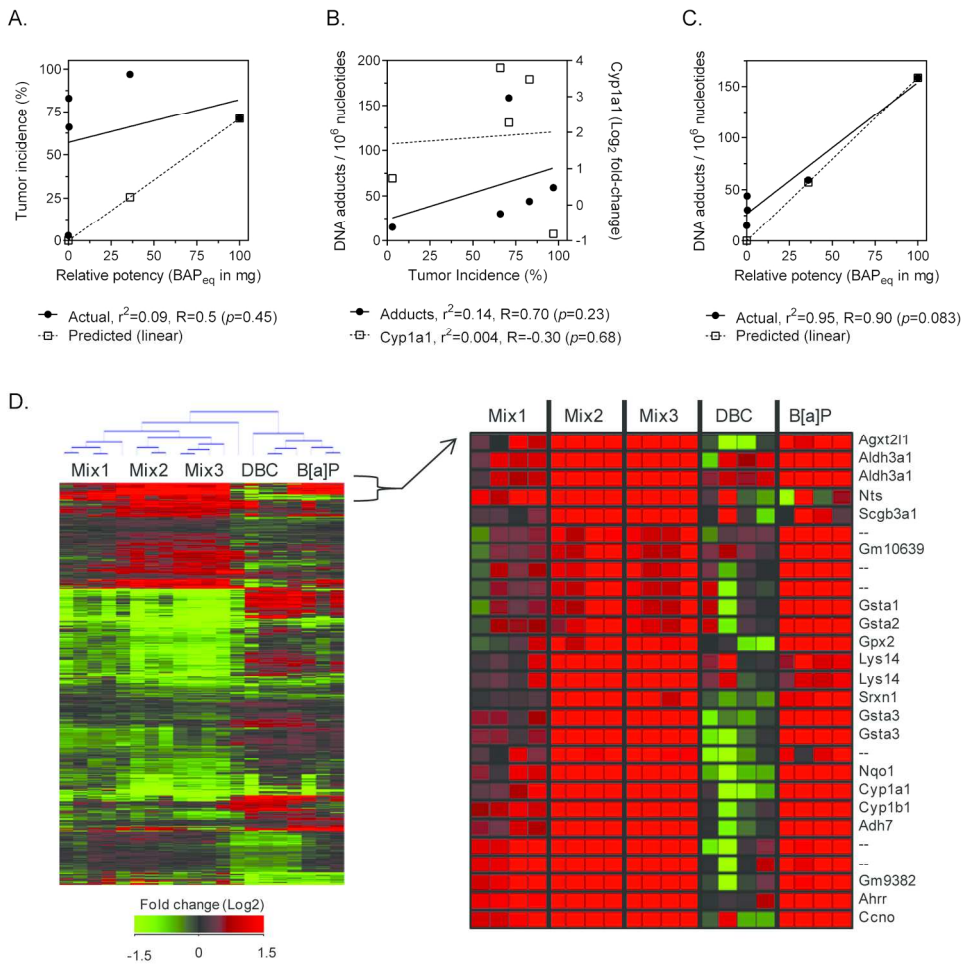
624

1
2
3
4
5
6
7
8
9
10
11
12
13
14
15
16
17
18
19
20
21
22
23
24
25
26
27
28
29
30
31
32
33
34
35
36
37
38
39
40
41
42
43
44
45
46
47
48
49
50
51
52
53
54
55
56
57
58
59
60



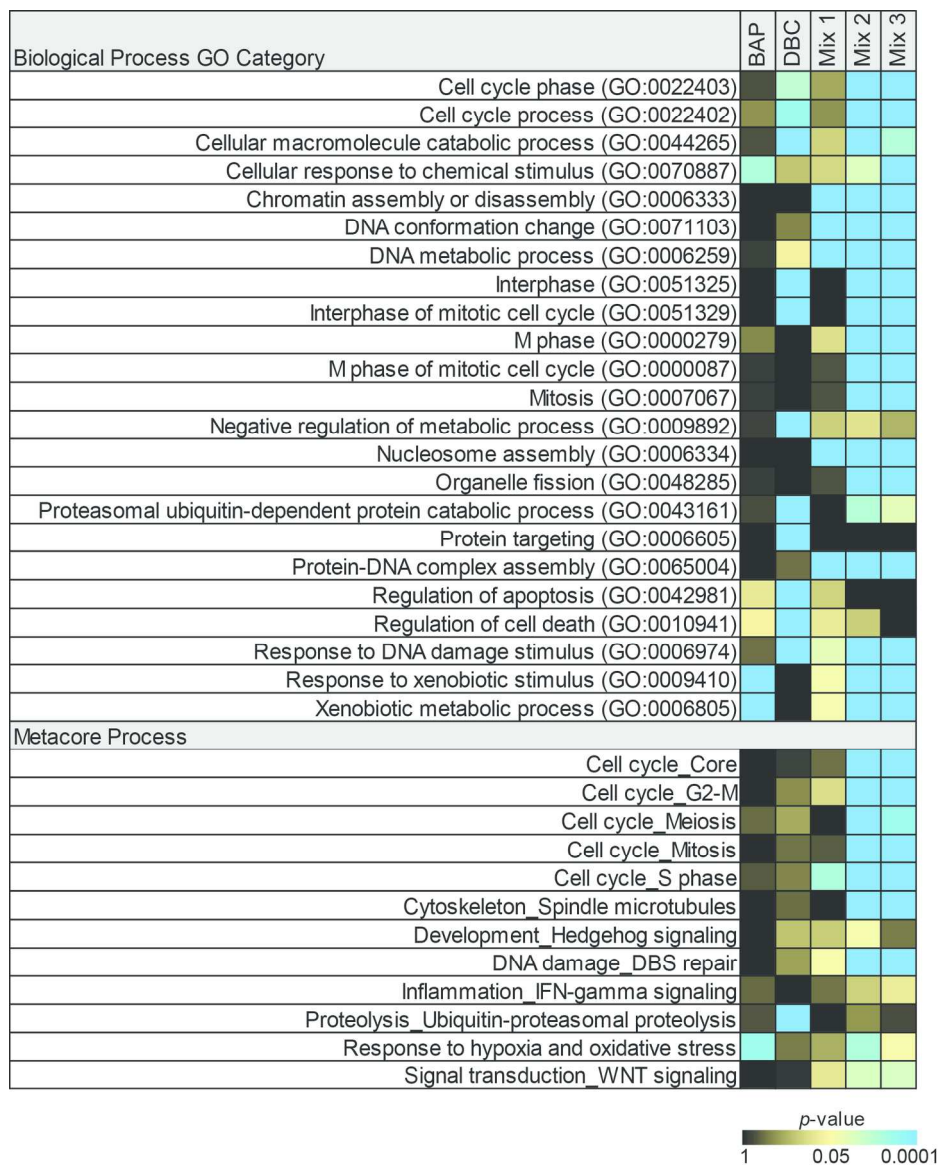
180x130mm (300 x 300 DPI)

1
2
3
4
5
6
7
8
9
10
11
12
13
14
15
16
17
18
19
20
21
22
23
24
25
26
27
28
29
30
31
32
33
34
35
36
37
38
39
40
41
42
43
44
45
46
47
48
49
50
51
52
53
54
55
56
57
58
59
60

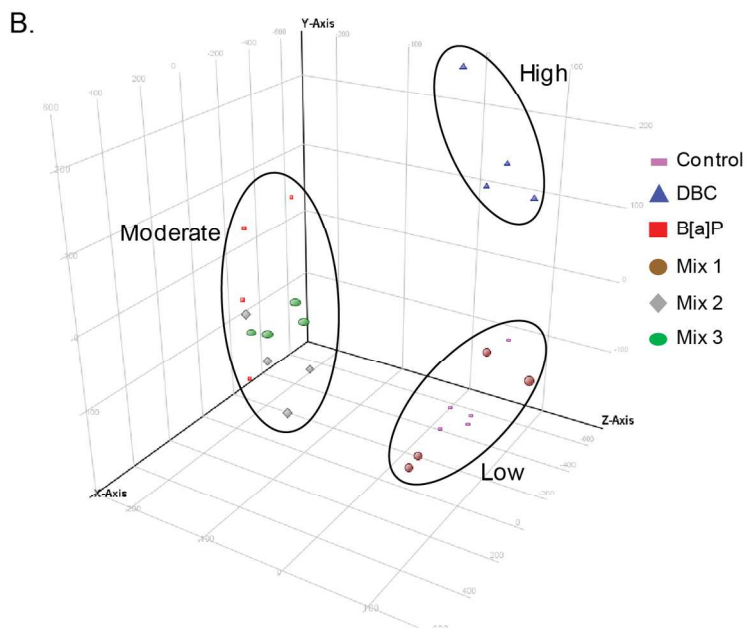
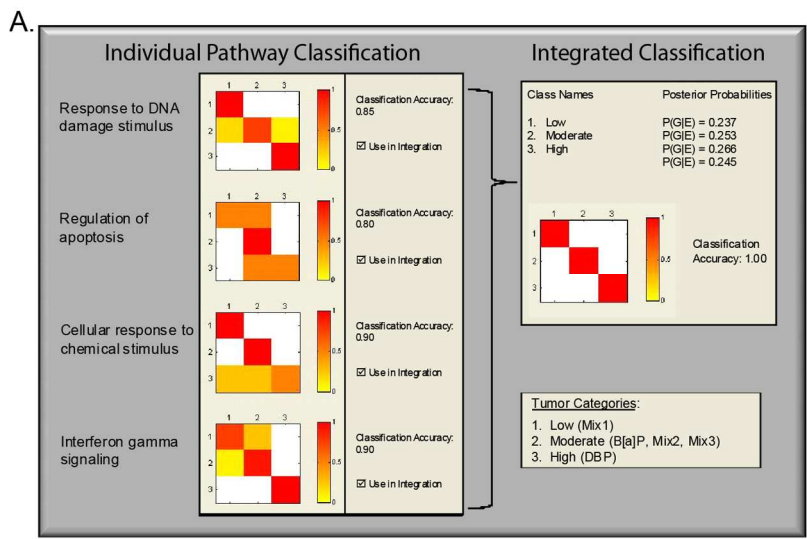


165x159mm (300 x 300 DPI)

1
2
3
4
5
6
7
8
9
10
11
12
13
14
15
16
17
18
19
20
21
22
23
24
25
26
27
28
29
30
31
32
33
34
35
36
37
38
39
40
41
42
43
44
45
46
47
48
49
50
51
52
53
54
55
56
57
58
59
60



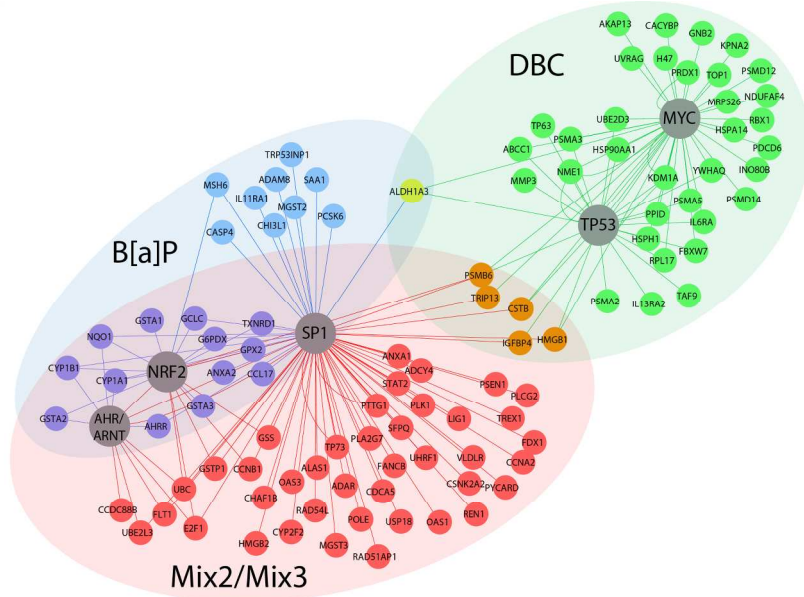
174x201mm (300 x 300 DPI)



120x181mm (300 x 300 DPI)

1
2
3
4
5
6
7
8
9
10
11
12
13
14
15
16
17
18
19
20
21
22
23
24
25
26
27
28
29
30
31
32
33
34
35
36
37
38
39
40
41
42
43
44
45
46
47
48
49
50
51
52
53
54
55
56
57
58
59
60

1
2
3
4
5
6
7
8
9
10
11
12
13
14
15
16
17
18
19
20
21
22
23
24
25
26
27
28
29
30
31
32
33
34
35
36
37
38
39
40
41
42
43
44
45
46
47
48
49
50
51
52
53
54
55
56
57
58
59
60



201x121mm (300 x 300 DPI)